Arabidopsis ADR1 helper NLR immune receptors localize and function at the plasma membrane in a phospholipid dependent manner

Svenja C. Saile[1], Frank M. Ackermann[1], Sruthi Sunil[1], Jutta Keicher[1], Adam Bayless[2], Vera Bonardi[3], Li Wan[3], Mehdi Doumane[4], Eva Stöbbe[1], Yvon Jaillais[4], Marie-Cécile Caillaud[4], Jeffery L. Dangl[3,5], Marc T. Nishimura[2], Claudia Oecking[1] and Farid El Kasmi*[,1]

Supporting Information

includes: -Supplementary Figure legends
-Supplementary Tables S1 and S2
-Supplementary Figures S1 – S11

Supplementary Figure legends

Fig. S1 Subcellular localization of AtADR1 proteins after transient over-expression in *N. benthamiana.*

Maximum projection of Z-stack images clearly demonstrates that AtADR1 proteins localize to the plasma membrane after transient expression in *N. benthamiana* leaves. (**a, b, e, f, g, h**) AtADR1 proteins (ADR1, ADR1-L1, ADR1-L2) localize mainly to the plasma membrane. The indicated ADR1 proteins fused to EYFP or Citrine-HA were transiently co-expressed with the PM-resident BRI1-mRFP fusion-protein and confocal imaging was done at 4 hours (**a, b, f**) or 5 hours (**h**) post Estradiol induction or 2 days post infiltration (**e, g**). (**c, d**) ADR1 also localizes to the endoplasmic reticulum (ER). Wildtype ADR1 or the autoactivated mutant ADR1^{DV} fused to Citrine-HA was transiently co-expressed with the ER-localized AtVMA12-RFP fusion-protein and confocal imaging was done at 3 hours (**c**) and 4 hours (**d**) post Estradiol induction. ADR1, ADR1^{DV} and ADR1-L1^{DV} additionally localize to puncta (white arrowheads in **a, b, c, d, f**). Localization of EYFP and Citrine-HA tagged ADR1 proteins is shown with the first column (Citrine/YFP, in yellow) and the co-localized PM-localized BRI1-mRFP or ER-localized VMA12-RFP is shown in the second column (RFP, in magenta). Chloroplasts are shown in the third column (Chlorophyll A, in cyan) and the merged images are shown in the fourth column. Images shown here are a maximum projection of Z-stack images. Scale bars, 20 µm.

Fig. S2 Subcellular localization of native promoter-driven AtADR1 proteins.

(**a-c**) Single plane secant views show that AtADR1 proteins (ADR1, ADR1-L1, ADR1-L2) localize to the plasma membrane (PM) when expressed under control of their native promoters. The indicated ADR1 proteins fused to YFP/EYFP were transiently co-expressed with the PM-resident protein BRI1-mRFP in *N. benthamiana* leaves and confocal imaging was done 3 days post infiltration (dpi; **a**) or 2 dpi (**b, c**). Localization of ADR1s is shown with the first column (YFP, in yellow) and the co-localized PM-resident BRI1 is shown in the second column (RFP, in magenta). Chloroplasts are shown in the third column (Chlorophyll A, in cyan) and the merged images are shown in the fourth column (merge). Fluorescence intensities were measured along the dotted line depicted in the merge images. Scale bars, 20 µm. (**d, e**) Subcellular fractionation experiments of protein extracts prepared from 7-day old *A. thaliana* seedlings stably expressing AtADR1-L2-HA under control of its native promoter (**d**) or from 6-week-old *A. thaliana* plants stably expressing AtADR1-L2^{DV}-HA under control of its native

promoter (**e**) reveal a strong membrane association of AtADR1-L2-HA (**d**) and ADR1-L2^{DV} (**e**). Shown are immunoblots of ADR1-L2-HA (**d**) and ADR1-L2^{DV}-HA (**e**) and the cytosolic marker UDP-glucose pyrophosphorylase (UGPase) using anti-HA or anti-UGPase antibody, respectively. 20 µg (**d**) or 40 µg (**e**) protein of each protein fraction (total, soluble, microsomes) was used for SDS-PAGE. Numbers show quantification of band intensities normalized to the band of the total protein fractions, respectively. T: total extract, S: soluble protein fraction, M: microsomal protein fraction.

Fig. S3 Characterization of the cell death activity of WT, P-loop and QHD variants of AtADR1s.

Transient expression of AtADR1s steady-state (WT), P-loop mutant (AAA) or QHD mutant (DV) Citrine-HA fusion proteins in *N. benthamiana*. ADR1, ADR1^{AAA} and ADR1^{DV} induce a strong HR-like cell death, whereas ADR1-L1^{DV} triggers a weak and ADR1-L2^{DV} a very weak HR-like cell death. Photos were taken under normal light at 23 hours post Estradiol induction and 47 hours post infiltration. Numbers represent the number of leaves showing cell death out of the number of leaves analysed. Asterisk indicates weak cell death, double-asterisk indicates very weak cell death.

Fig. S4 AtRPS5 plasma membrane localization and its cell death activity are not affected by MAP-SAC1 or MAP-dOCRL co-expression.

(**a**) Plasma membrane localization of AtRPS5-EYFP is not affected by co-expression of MAP-mCherry-SAC1^{dead} (upper panel) or MAP-mCherry-SAC1^{WT} (lower panel). (**c**) Co-expression of MAP-mCherry-dOCRL^{dead} (upper panel) or MAP-mCherry-dOCRL^{WT} (lower panel) does not affect RPS5-EYFP PM localization. Indicated proteins were transiently expressed in *N. benthamiana* leaves and confocal imaging was done at 24 hours post infiltration. Localization of RPS5-EYFP is shown with the first column (YFP, in yellow) and MAP-mCherry-SAC1^{WT}, MAP-mCherry-SAC1^{dead}, MAP-mCherry-dOCRL^{dead} and MAP-mCherry-dOCRL^{WT} are shown in the second column (mCherry, in magenta). Chloroplasts are shown in the third column (Chlorophyll A, in cyan) and the merged images are shown in the fourth column (merge). Images are single plane secant views. Scale bars, 20 µm. (**b, d**) Immunoblot analysis of the transiently expressed proteins (see (**a**, **c**)) using anti-GFP and anti-RFP antibody, respectively. Equal loading of the proteins is indicated by the Rubisco band from the Ponceau staining (PS). Numbers show quantification of band intensities normalized to the Rubisco band from the Ponceau staining. Samples were collected 24 hours post infiltration. (**e, f**) Effector

(AvrPphB)-triggered and RPS5-EYFP mediated cell death is not suppressed by MAP-mCherry-SAC1^{WT} (**e**) or MAP-mCherry-dOCRL^{WT} (**f**) co-expression in *N. benthamiana*. Leaf images showing cell death induction by activated RPS5-EYFP (upper panels). Transient expression of the Dexamethasone-inducible effector AvrPphB-MYC and the guardee protein PBS1-HA with constitutively expressed RPS5-EYFP, MAP-mCherry-SAC1^{WT} or MAP-mCherry-SAC1^{dead} (**e**) or MAP-mCherry-dOCRL^{dead} and MAP-mCherry-dOCRL^{WT} (**f**). Leaf images were taken under UV light at 24 hours post Dexamethasone induction, which corresponds to 2 days post infiltration (**e, f**). AvrPphB-MYC and PBS1-HA expression was induced with 30 µM Dexamethasone to activate RPS5-EYFP. White/light grey areas indicate dead leaf tissue. Numbers represent the number of leaves showing cell death out of the number of leaves analysed. Immunoblot analysis (lower panels) of the transiently expressed proteins (see upper panels) using anti-GFP and anti-RFP antibody, respectively. Equal loading of the proteins is indicated by the Rubisco band from the Ponceau staining (PS). Numbers show quantification of band intensities normalized to the Rubisco band from the Ponceau staining. Protein samples were collected at 6 hours post Dexamethasone induction, which corresponds to 28 hours post infiltration.

Fig. S5 Degradation of mis-localized AtRPM1 and AtADR1 proteins is not or only partially blocked by proteasome inhibitors.

(**a-c**) Treatment of a 1x Protease Inhibitor Cocktail (PIC) or 2.5 µM Bortezomib (BTZ) fully (**a**) or partially (**b, c**) inhibit the degradation of mis-localized AtADR1 proteins. (**d**) Mis-localized AtRPM1 protein degradation can partially be blocked by a PIC treatment, however not by BTZ. Shown are anti-GFP immunoblots of AtADR1 (**a**), AtADR1-L1 (**b**), AtADR1-L2 (**c**) and AtRPM1 (**d**) Citrine-HA or EYFP fusion proteins that were transiently co-expressed with MAP-mCherry-SAC1^{WT} or MAP-mCherry-SAC1^{dead} in *N. benthamiana*. Equal loading of the proteins is indicated by the Rubisco band from the Ponceau staining (PS). Numbers show quantification of band intensities normalized to the Rubisco band from the Ponceau staining. Samples were collected 4 hours (**a**) or 5 hours (**b-d**) post inhibitor and Estradiol (**a**) treatments, which corresponds to 27 (**a**) and 25 hours (**b-d**) post infiltration.

Fig. S6 Effector-triggered AtRPM1-mediated cell death response is diminished by PI4P depletion.

(**a**, upper panel) CC_R domain of AtADR1-L1 induces no visible cell death symptoms and thus no effect of MAP-mCherry-SAC1^{WT} co-expression on AtADR1-L1 CC_R activity is observable. Transient co-expression of ADR1-L1 CC_R-EYFP, MAP-mCherry-SAC1^{WT} or MAP-mCherry-SAC1^{dead} in *N. benthamiana* leaves. (**b**, upper panel) mCherry-SAC1^{WT} co-expression noticeably reduced cell death activity of AvrRpm1-HA activated RPM1-EYFP. Transient expression of RPM1-EYFP, AvrRPM1-HA, T7-RIN4 and MAP-mCherry-SAC1^{WT} or MAP-mCherry-SAC1^{dead} in *N. benthamiana* leaves. (**c**, upper panel) Cell death activity of AvrRpm1-HA activated RPM1-EYFP was not blocked by co-expression of MAP-mCherry-dOCRL^{dead} or MAP-mCherry-dOCRL^{WT}. Transient expression of RPM1-EYFP, AvrRPM1-HA, T7-RIN4 and MAP-mCherry-dOCRL^{dead} or MAP-mCherry-dOCRL^{WT} in *N. benthamiana* leaves. AvrRPM1-HA expression was induced with 30 µM Dexamethasone 20 hours post infiltration. Leaf images were taken under UV light at 24 hours post infiltration (**a**) or 24 hours post Dexamethasone induction (**b**, **c**). The effector AvrRpm1 and the guardee protein RIN4 was co-expressed to activate RPM1. White/light grey areas indicate dead leave tissue. Numbers represent the number of leaves showing cell death out of the number of leaves analysed. Asterisk in (**b**) indicates weak cell death. (**a-c**, lower panels) Immunoblot analysis of the proteins transiently expressed in leaves (see upper panels) using anti-GFP and anti-RFP antibody, respectively. Equal loading of the proteins is indicated by the Rubisco band from the Ponceau staining (PS). Numbers show quantification of band intensities normalized to the Rubisco band from the Ponceau staining. Protein samples were collected at 20 hours post infiltration (**a**) and 6 hours post Dexamethasone induction, which corresponds to 26 hours post infiltration (**b, c**).

Fig. S7 PI4P depletion affects the PM localization of AtADR1 CC_R domains.

Co-expression with SAC1^{WT} affects AtADR1 CC_R (**a**), AtADR1-L1 CC_R (**b**) and AtADR1-L2 CC_R (**c**) localization. C-terminally Citrine-HA tagged AtADR1 (ADR1, ADR1-L1, ADR1-L2) CC_R domains were transiently co-expressed with MAP-mCherry-SAC1^{dead} (**a-c**, upper panel) or MAP-mCherry-SAC1^{WT} (**a-c**, lower panel) in *N. benthamiana* leaves. Confocal imaging was done at 3 hours (**a**) or 4 hours after Estradiol induction (**b, c**). AtADR1 CC_R, AtADR1-L1 CC_R and AtADR1-L2 CC_R domains re-localize to intracellular puncta (white arrow heads), potentially endosomes. Localization of AtADR1 CC_R-Citrine-HA domains is shown with the first column (Citrine, in yellow) and MAP-mCherry-SAC1^{WT} or MAP-mCherry-SAC1^{dead} is shown in the second column (mCherry, in magenta). Chloroplasts are shown in the third

column (Chlorophyll A, in cyan) and the merged images are shown in the fourth column (merge). Images shown here are a maximum projection of Z-stack images. Scale bars, 20 µm.

Fig. S8 $PI(4,5)P_2$ is not required for the PM localization and stability of AtADR1s and AtRPM1.

(**a, c, e, g**) Plasma membrane localization of AtADR1s (ADR1-Citrine-HA, ADR1-L1-EYFP, ADR1-L2-EYFP) and AtRPM1-EYFP is not altered when $dOCRL^{dead}$ (upper panel) or $dOCRL^{WT}$ (lower panel) is co-expressed. Proteins were transiently expressed in *N. benthamiana* leaves and confocal imaging was done 3 hours post Estradiol induction (**a**), 2 days post infiltration (**c, e**) or 24 hours post infiltration (**g**). Localization of Citrine-HA/-EYFP tagged ADR1s and RPM1-EYFP is shown with the first column (Citrine/YFP, in yellow) and MAP-mCherry-$dOCRL^{WT}$ or MAP-mCherry-$dOCRL^{dead}$ is shown in the second column (mCherry, in magenta). Chloroplasts are shown in the third column (Chlorophyll A, in cyan) and the merged images are shown in the fourth column (merge). Images are single plane secant views. Scale bars, 20 µm. (**b, d, f, h**) Immunoblot analysis of transiently expressed proteins (see (**a**), (**c**), (**e**), (**g**)) using anti-GFP and anti-RFP antibody, respectively, show no effect on NLR stability by $dOCRL^{WT}$ or $dOCRL^{dead}$ co-expression. Equal loading of proteins is indicated by the Rubisco band from the Ponceau staining (PS). Numbers show quantification of band intensities normalized to the Rubisco band from the Ponceau staining. Samples were collected at 4 hours post Estradiol induction (**b**), 2 days post infiltration (**d, f**) or 24 hours post infiltration (**h**).

Fig. S9 AtADR1s and AtRPM1 cell death activity is not affected by depletion of $PI(4,5)P_2$ from the plasma membrane via MAP-dOCRL co-expression.

$dOCRL^{WT}$ co-expression does not affect the cell death induced by AtADR1 CC_R (**a**), AtADR1-L2 CC_R (**b**), AtNRG1.1 CC_R (**c**) domains, full-length AtADR1 (**d**), autoactive mutant $AtADR1^{DV}$ (**e**) or activated AtRPM1 (**f**). (**a-f**, upper panels) Transient expression of Citrine-HA or EYFP tagged ADR1 (**d**), autoactive $ADR1^{D461V}$ mutant (**e**) and phospho-mimic T7-$RIN4^{T166D}$-activated RPM1 (**f**) co-expressed with MAP-mCherry-dOCRLWT or MAP-mCherry-$dOCRL^{dead}$ in *N. benthamiana*. Leaf images were taken under UV light at 24 hours post infiltration (hpi) (**a**), 26 hpi (**b**), 28 hpi (**c**), 9 hours post Estradiol induction (**d**), 30 hpi (**e**) and 24 hpi (**f**). Phospho-mimic T7-$RIN4^{T166D}$ ($RIN4^{TD}$) was co-expressed to activate RPM1. White/light grey areas in leaves indicate dead tissue. Numbers represent the number of leaves showing cell death out of the number of leaves analysed. Asterisk indicates weak HR. (**a-f**,

lower panels) Immunoblot analysis of transiently expressed proteins (see upper panels) using anti-GFP and anti-RFP antibody, respectively. Equal loading of proteins is indicated by the Rubisco band from the Ponceau staining (PS). Numbers show quantification of band intensities normalized to the Rubisco band from the Ponceau staining. Samples were collected at 20 hpi (**a-c**), 24 hpi (**d**), 4 hours post Estradiol induction (**e**) or 22 hpi (**f**).

Fig. S10 Basic-hydrophobic (BH) profile analysis of CC/CC$_R$ domains.

In silico analysis to identify potential basic-hydrophobic stretches in the CC/CC$_R$ domains of three Arabidopsis CNLs and the whole RNL family. (**a**) BH score profile (window size 19) of AtADR1, AtADR1-L1, AtADR1-L2, AtRPM1, AtZAR1, AtNRG1.1, AtNRG1.2 and AtRPS5 CC/CC$_R$ domains (amino acids 1-160/170). Potential BH-stretches are represented as peaks above the 0.6 BH score threshold shown as a green line. Isoelectric point (pI) of each CC/CC$_R$ domain is shown in parentheses behind the protein names and indicates that all but two (RPM1 and ZAR1) CC and CC$_R$ domains may have an overall positive charge in the cytosolic environment (pH ~7.2). (**b**) Amino acid sequences of CC and CC$_R$ domains as in (**a**) with the putative BH-stretch indicated by italic, underlined letters and highlighted in yellow. Positively charged lysine (K) and arginine (R) residues in the BH-stretch are shown in bold and red letters.

Fig. S11 Proposed model of AtADR1 family members localization, oligomerization and function during immunity.

Arabidopsis ADR1s constitutively localize at the plasma membrane through the interaction of their CC$_R$ domains with anionic lipids, including PI4P. AtADR1 activation, either by pathogen infection or autoactivating mutations, leads to (**1**) conformational changes inducing or strengthening oligomerization andthe formation of a transient Ca^{2+}-permeable cation channel that results in (**2**) Ca^{2+} influx and in the (**3**) subsequent recruitment or activation of calcium dependent and probably NLR-interacting phospholipases that (**4**) in turn produce lipid messengers, such as PA and DAG, which (**5**) might activate downstream signalling components required for NLR-mediated (**6**) immunity. The lipase-like protein AtEDS1 (ENHANCED DISEASE SUSCEPTIBLE 1) and its sequence-related direct partner AtPAD4 (PHYTOALEXIN DEFICIENT 4) are key immune regulators of AtADR1s-mediated immunity, but also of basal resistance, and may be part of an ADR1s immune-signalling complex.

Table S1. Transmembrane domain and lipidation prediction summary for *Arabidopsis thaliana* RNLs and the CNLs RPM1 and RPS5.

NLR (type)	TMD prediction*		Lipidation prediction*		
	Tool	result	Tool	# of sites	position in protein
AtRPM1 (CNL) At3g07040	TMHMM2.0	no	NBA-Palm		0
	CCTOP	no	GPS-Palm	3	438,567,704
	PredictProtein	no	ExPASy Myristoylator		0
AtRPS5 (CNL) At1g12220	TMHMM2.0	no	NBA-Palm		0
	CCTOP	no	GPS-Palm	4	**4**,103,106,463
	PredictProtein	no	ExPASy Myristoylator	1	N-terminus
AtADR1 (RNL) At1g33560	TMHMM2.0	no	NBA-Palm		0
	CCTOP	no	GPS-Palm	1	661
	PredictProtein	no	ExPASy Myristoylator		0
AtADR1-L1 (RNL) At4g33300	TMHMM2.0	no	NBA-Palm		0
	CCTOP	no	GPS-Palm	4	301,347,638,690
	PredictProtein	no	ExPASy Myristoylator		0
AtADR1-L2 (RNL) At5g04720	TMHMM2.0	no	NBA-Palm		0
	CCTOP	no	GPS-Palm	2	73,685
	PredictProtein	no	ExPASy Myristoylator		0
AtNRG1.1 (RNL) At5g66900	TMHMM2.0	no	NBA-Palm		0
	CCTOP	no	GPS-Palm	5	198,592,683,705,731
	PredictProtein	no	ExPASy Myristoylator		0
AtNRG1.2 (RNL) At5g66910	TMHMM2.0	no	NBA-Palm		0
	CCTOP	no	GPS-Palm	6	200,598,689,711,737,764
	PredictProtein	no	ExPASy Myristoylator		0

*, web-pages of the used prediction tools are listed in the Material and Methods section.

Table S2. Primer list.

Primer	sequence	purpose
FEK_1014	GACGCAACACGtTGTTTTGAGAGACCTAG	ADR1 D461V (site-directed mutagenesis)
FEK_1015	CTAGGTCTCTCAAAACAaCGTGTTGCGTC	ADR1 D461V (site-directed mutagenesis)
FEK_1012	GTGACACAGCATGtTGTTCTGCGAGAC	ADR1-L1 D489V (site-directed mutagenesis)
FEK_1013	GTCTCGCAGAACAaCATGCTGTGTCAC	ADR1-L1 D489V (site-directed mutagenesis)
FEK_948	GTCACGCAGCATGtTGTTCTAAGAGATG	ADR1-L2 D484V (site-directed mutagenesis)

FEK_949	CATCTCTTAGAACAaCATGCTGCGTGAC	ADR1-L2 D484V (site-directed mutagenesis)
FEK_1002	GAATGAGCGGTTCAGcGgcAgCCACTCTTG	ADR1 198AAA200 (site-directed mutagenesis)
FEK_1003	CAAGAGTGGcTgcCgCTGAACCGCTCATTC	ADR1 198AAA200 (site-directed mutagenesis)
FEK_1000	GAATGGGCGGTGTTGcTgcAgCCACTCTTGCC	ADR1-L1 212AAA214 (site-directed mutagenesis)
FEK_1001	GGCAAGAGTGGcTgcAgCAACACCGCCCATTC	ADR1-L1 212AAA214 (site-directed mutagenesis)
FEK_973	GGATGAGTGGTTCAGcGgcAgCCACTCTTG	ADR1-L2 212AAA214 (site-directed mutagenesis)
FEK_974	CAAGAGTGGcTgcCgCTGAACCACTCATCC	ADR1-L2 212AAA214 (site-directed mutagenesis)
FEK_1475	gtGGTCTCaGCGGGCTAACTTATGTTGACTTCACGA	ADR1 promoter with *Bsa*I site and GCGG overhang (GG)
FEK_1476	atGGTCTCaCAGACGAGACCGATCTTGGAGTGTAAG	ADR1 promoter with *Bsa*I site and GCGG overhang (GG)
FEK_1477	gtGGTCTCaTCTGATGGCTTCGTTCATAGATCTTTTCG	ADR1 CDS with *Bsa*I site and TCTG overhang (GG)
FEK_1478	atGGTCTCaCCTTATCGTCAAGCCAATCCACGGTGAAGC	ADR1 CDS with *Bsa*I site and CCTT overhang and w/o stop (GG)
FEK_1420	GGGGACAAGTTTGTACAAAAAAGCAGGCTTActccactcatggcagcaatact	ADR1-L1 promoter with attB1 site (GW)
FEK_1421	GGTGATGGCCATtggataccaccaagtcaagtc	ADR1-L1 promoter with ADR1-L1 CDS overhang
FEK_1422	gtggtatccaATGGCCATCACCGATTTTTTCG	ADR1-L1 CDS with ADR1-L1 promoter overhang

FEK_1423	GGGGACCACTTTGTACAAGAAAGCTGGGTGTTCGTCAAGCCAGTCTAGG	ADR1-L1 CDS with attB2 site
PMNLR_013	GGGGACAAGTTTGTACAAAAAAGCAGGCTtaATGGGAGGTTGTTTCTCTGTTTCATTGCC	RPS5 forward primer for pDONOR gateway cloning
PMNLR_014	GGGGACCACTTTGTACAAGAAAGCTGGGTtTGTTTCTCTCCACCGCCACCTGGATGAAGG	RPS5 reward primer for pDONOR gateway cloning
FEK_1311	cgtagatctatttaggtgacactatagaacag*accacc*ATGGCTTCGGCTACTGTTGATTTT	SP6 RPM1 CC 1-156 (TnT)
FEK_1312	cgtagatcCTAAGCGTAATCTGGAACGTCATATGGATACTTTGCATCGCCATCATCAAT	1xHA rev for RPM1 CC 1-156 (TnT)
FEK_1329	cgtagatctatttaggtgacactatagaacag*accacc*ATGGCTTCGTTCATAGATC	SP6 ADR1 CC 1-146 (TnT)
FEK_1330	cgtagatcCTAAGCGTAATCTGGAACGTCATATGGATAATCATTCCGCTCAGTCAAC	1xHA rev for ADR1 CC 1-146 (TnT)
FEK_1331	cgtagatctatttaggtgacactatagaacag*accacc*ATGGCCATCACCGATTTTTTCG	SP6 ADR1-L1 CC 1-155 (TnT)
FEK_1332	cgtagatcCTAAGCGTAATCTGGAACGTCATATGGATATCCCCCAATTTTCATGGAAC	1xHA rev for ADR1-L1 CC 1-155 (TnT)
FEK_1313	cgtagatctatttaggtgacactatagaacag*accacc*ATGGCAGATATAATCGGCG	SP6 ADR1-L2 CC 1-153 (TnT)
FEK_1314	cgtagatcCTAAGCGTAATCTGGAACGTCATATGGATATCCCCTGAGTTTCATAGAACC	1xHA rev for ADR1-L2 CC 1-153 (TnT)
FEK_1425	cgtagatctatttaggtgacactatag*aacagaccacc*ATGGTGAGCAAGGGCGAG	SP6 Citrine (TnT)
FEK_1426	cgtagatcTCAGGCATAGTCTGGGACGTCATATGGATACTTG	1xHA rev for Citrine (TnT)
5phos	catcatactcctttgcctgctgccgctgccgctatggtgagcaagggcgaggagg	5' phosphorylated primers for MAP-mCherrynoSTOP/ pDONR207 cloning
5phos_R	TCGACTTCTACTGCAGAGTAAGCCCATGGTAGCCTGCTTTTTTGTACAAACTTGGC	5' phosphorylated primers for MAP-mCherrynoSTOP/ pDONR207 cloning

223

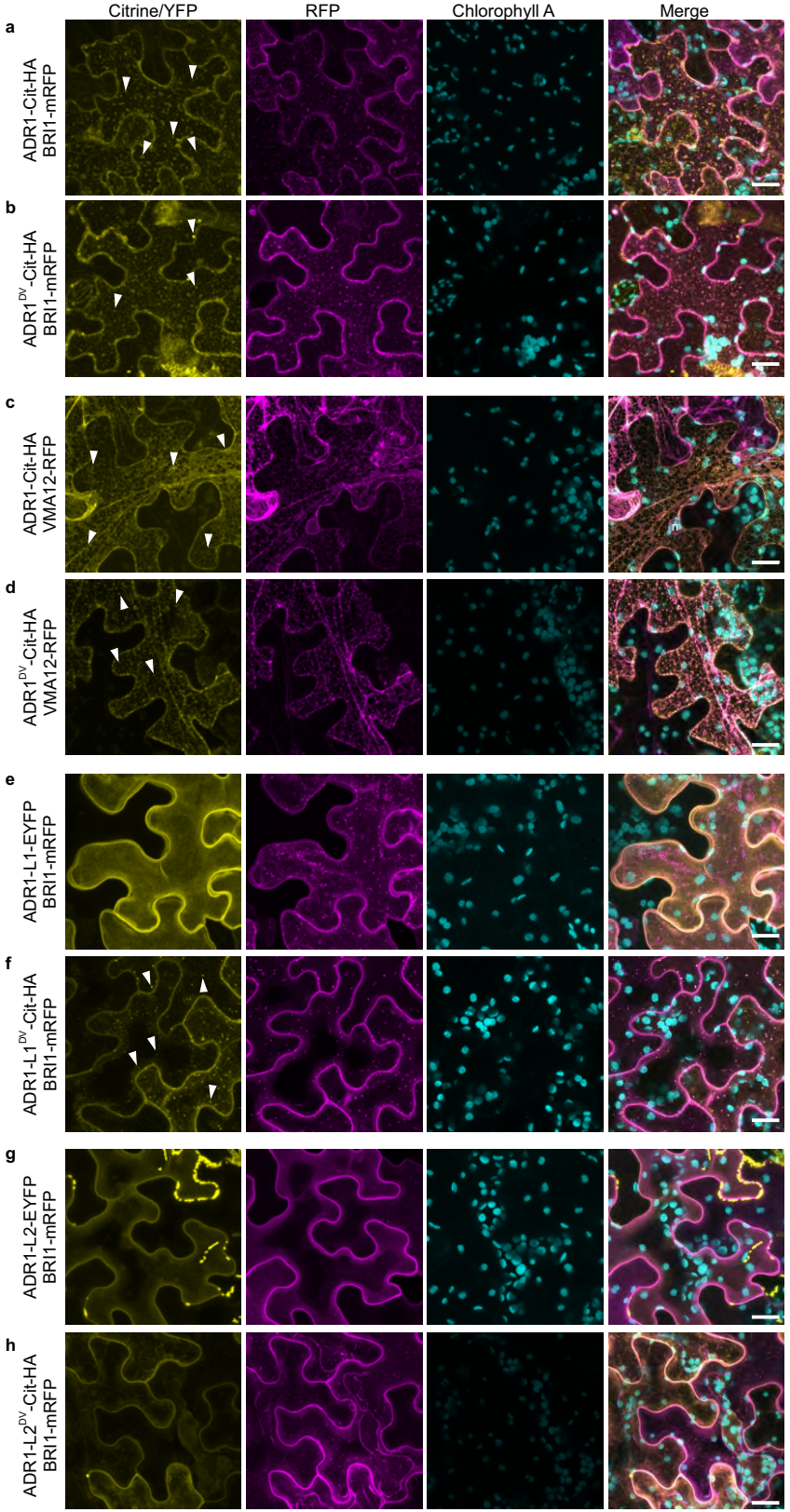
Citrine/YFP
RFP
Chlorophyll A
Merge
a
ADR1-Cit-HA
BRI1-mRFP
b
ADR1DV-Cit-HA
BRI1-mRFP
c
ADR1-Cit-HA
VMA12-RFP
n
d
ADR1DV-Cit-HA
VMA12-RFP
e
ADR1-L1-EYFP
BRI1-mRFP
f
ADR1-L1DV-Cit-HA
BRI1-mRFP
g
ADR1-L2-EYFP
BRI1-mRFP
h
ADR1-L2DV-Cit-HA
BRI1-mRFP

S1 Fig.

S2 Fig.

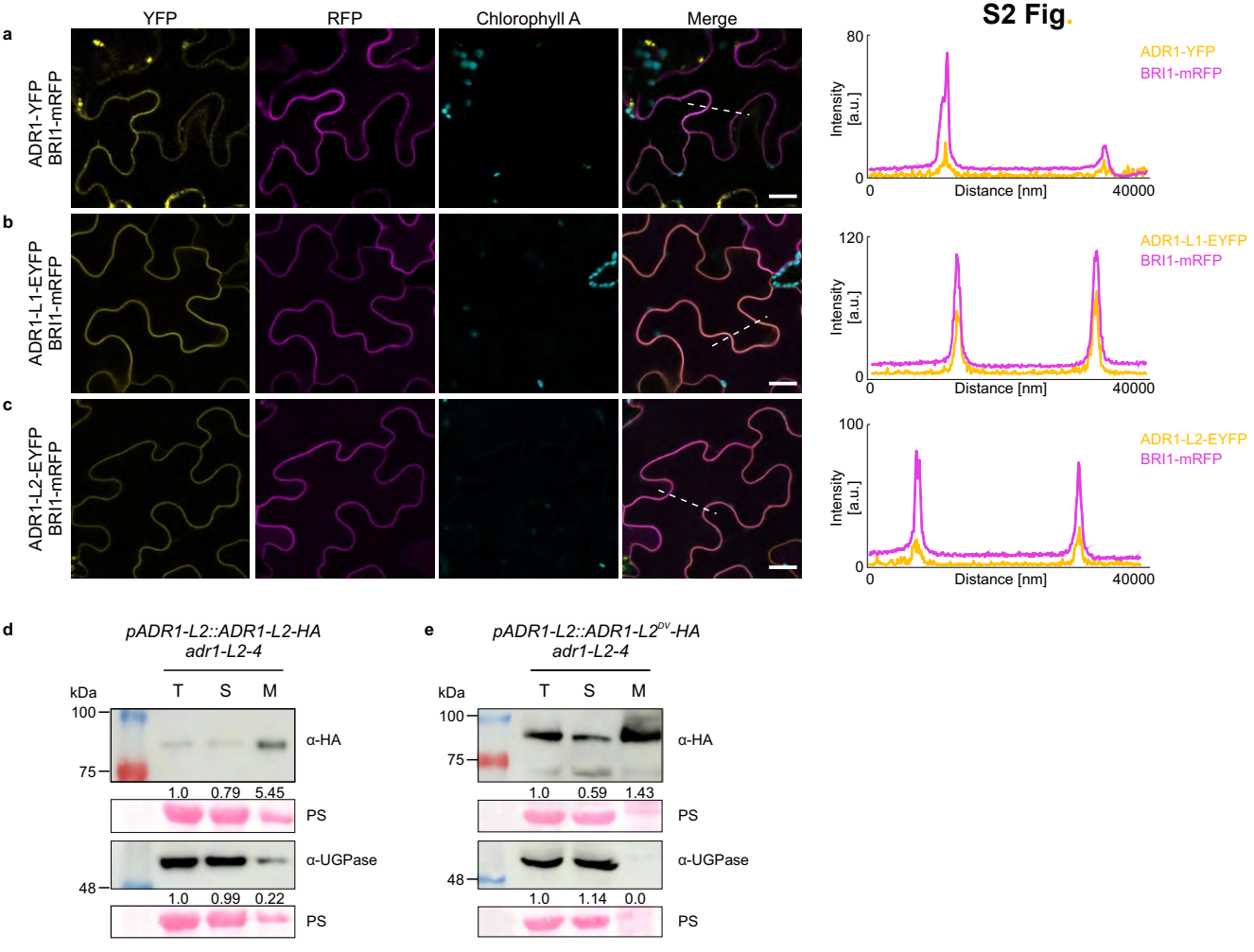
a
b
c
YFP
RFP
Chlorophyll A
Merge
ADR1-YFP
BRI1-mRFP
ADR1-L1-EYFP
BRI1-mRFP
ADR1-L2-EYFP
BRI1-mRFP
Intensity [a.u.]
Distance [nm]
0
40000
80
120
100
ADR1-YFP
BRI1-mRFP
ADR1-L1-EYFP
BRI1-mRFP
ADR1-L2-EYFP
BRI1-mRFP

d
pADR1-L2::ADR1-L2-HA
adr1-L2-4
kDa
T
S
M
100
75
48
α-HA
1.0
0.79
5.45
PS
α-UGPase
1.0
0.99
0.22
PS
e
pADR1-L2::ADR1-L2DV-HA
adr1-L2-4
kDa
T
S
M
100
75
48
α-HA
1.0
0.59
1.43
PS
α-UGPase
1.0
1.14
0.0
PS

S3 Fig.


ADR1WT
28/28
ADR1DV
28/28
ADR1AAA
8/8
ADR1-L1WT
0/26
ADR1-L1DV
24*/26
ADR1-L1AAA
0/6
ADR1-L2WT
0/26
ADR1-L2DV
13**/26
ADR1-L2AAA
2**/6

S4 Fig.

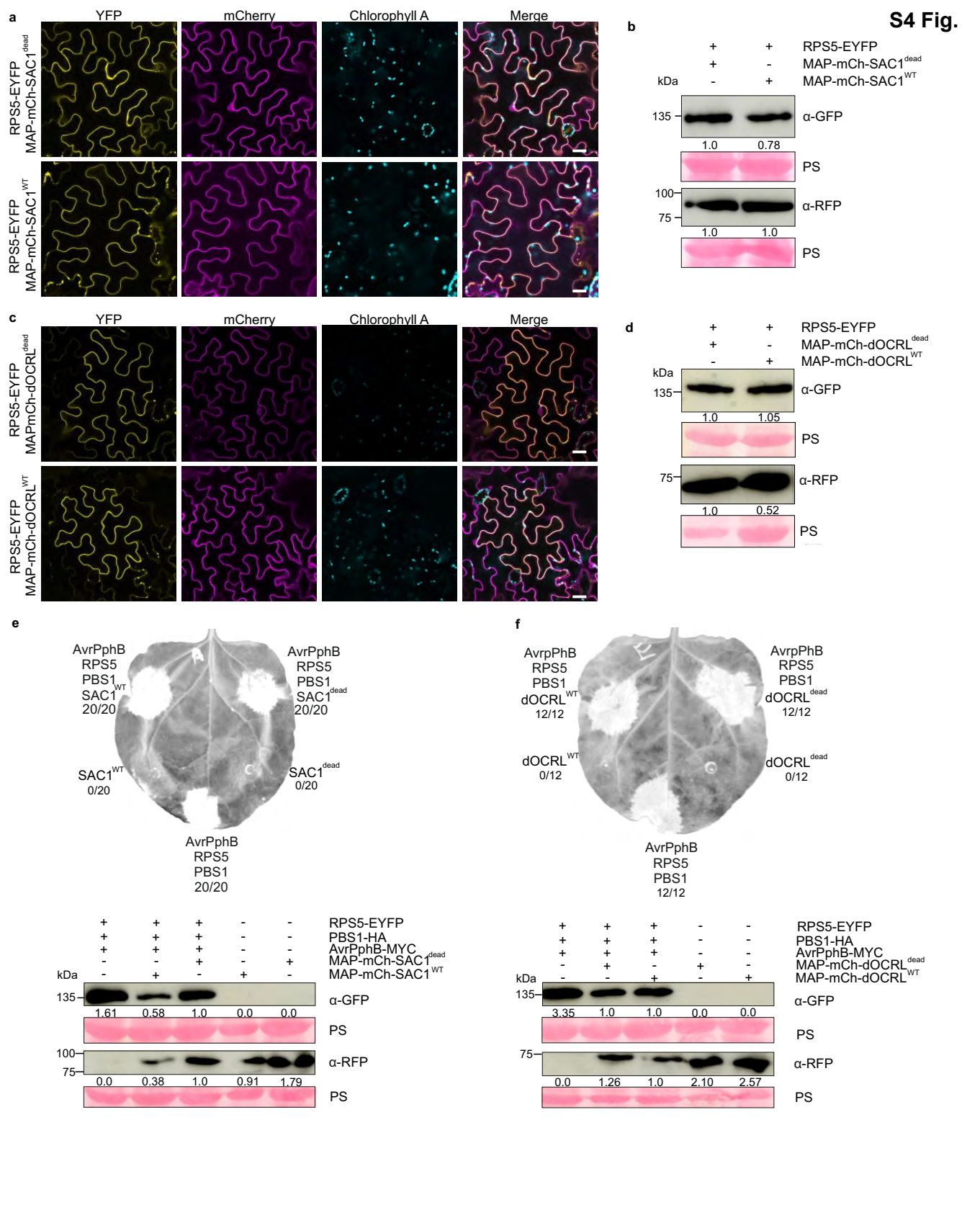
a
YFP
mCherry
Chlorophyll A
Merge
RPS5-EYFP
MAP-mCh-SAC1dead
RPS5-EYFP
MAP-mCh-SAC1WT
b
RPS5-EYFP
MAP-mCh-SAC1dead
MAP-mCh-SAC1WT
kDa
135
α-GFP
1.0 0.78
PS
100
75
α-RFP
1.0 1.0
PS
c
YFP
mCherry
Chlorophyll A
Merge
RPS5-EYFP
MAPmCh-dOCRLdead
RPS5-EYFP
MAP-mCh-dOCRLWT
d
RPS5-EYFP
MAP-mCh-dOCRLdead
MAP-mCh-dOCRLWT
kDa
135
α-GFP
1.0 1.05
PS
75
α-RFP
1.0 0.52
PS
e
AvrPphB
RPS5
PBS1WT
SAC1WT
20/20
AvrPphB
RPS5
PBS1
SAC1dead
20/20
SAC1WT
0/20
SAC1dead
0/20
AvrPphB
RPS5
PBS1
20/20
RPS5-EYFP
PBS1-HA
AvrPphB-MYC
MAP-mCh-SAC1dead
MAP-mCh-SAC1WT
kDa
135
α-GFP
1.61 0.58 1.0 0.0 0.0
PS
100
75
α-RFP
0.0 0.38 1.0 0.91 1.79
PS
f
AvrpPhB
RPS5
PBS1
dOCRLWT
12/12
AvrpPhB
RPS5
PBS1
dOCRLdead
12/12
dOCRLWT
0/12
dOCRLdead
0/12
AvrPphB
RPS5
PBS1
12/12
RPS5-EYFP
PBS1-HA
AvrPphB-MYC
MAP-mCh-dOCRLdead
MAP-mCh-dOCRLWT
kDa
135
α-GFP
3.35 1.0 1.0 0.0 0.0
PS
75
α-RFP
0.0 1.26 1.0 2.10 2.57
PS

S5 Fig.

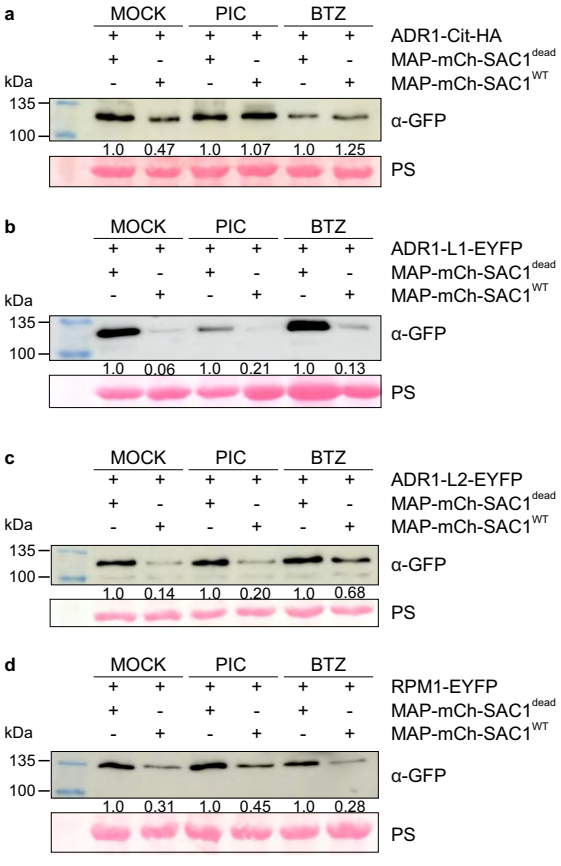
a
MOCK
PIC
BTZ
+ + + + + +
ADR1-Cit-HA
+ - + - + -
MAP-mCh-SAC1dead
- + - + - +
MAP-mCh-SAC1WT
kDa
135
100
α-GFP
1.0 0.47 1.0 1.07 1.0 1.25
PS
b
MOCK
PIC
BTZ
+ + + + + +
ADR1-L1-EYFP
+ - + - + -
MAP-mCh-SAC1dead
- + - + - +
MAP-mCh-SAC1WT
kDa
135
100
α-GFP
1.0 0.06 1.0 0.21 1.0 0.13
PS
c
MOCK
PIC
BTZ
+ + + + + +
ADR1-L2-EYFP
+ - + - + -
MAP-mCh-SAC1dead
- + - + - +
MAP-mCh-SAC1WT
kDa
135
100
α-GFP
1.0 0.14 1.0 0.20 1.0 0.68
PS
d
MOCK
PIC
BTZ
+ + + + + +
RPM1-EYFP
+ - + - + -
MAP-mCh-SAC1dead
- + - + - +
MAP-mCh-SAC1WT
kDa
135
100
α-GFP
1.0 0.31 1.0 0.45 1.0 0.28
PS

S6 Fig.

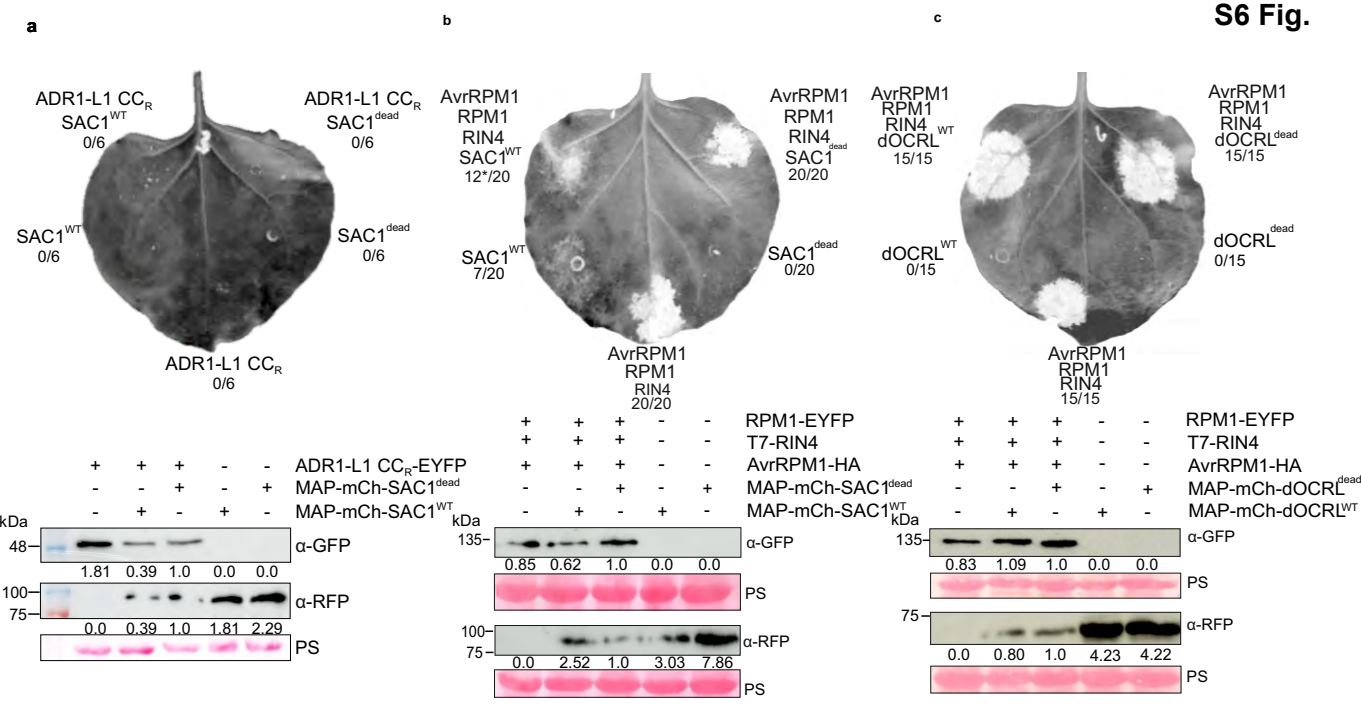
a
ADR1-L1 CC$_R$
SAC1^{WT}
0/6
ADR1-L1 CC$_R$
SAC1^{dead}
0/6
SAC1^{WT}
0/6
SAC1^{dead}
0/6
ADR1-L1 CC$_R$
0/6
b
AvrRPM1
RPM1
RIN4
SAC1^{WT}
12*/20
AvrRPM1
RPM1
RIN4$_{dead}$
SAC1^{dead}
20/20
SAC1^{WT}
7/20
SAC1^{dead}
0/20
AvrRPM1
RPM1
RIN4
20/20
c
AvrRPM1
RPM1
RIN4
dOCRL^{WT}
15/15
AvrRPM1
RPM1
RIN4
dOCRL^{dead}
15/15
dOCRL^{WT}
0/15
dOCRL^{dead}
0/15
AvrRPM1
RPM1
RIN4
15/15
+ + + - - ADR1-L1 CC$_R$-EYFP
- - + - + MAP-mCh-SAC1^{dead}
- + - + - MAP-mCh-SAC1^{WT}
kDa
48
α-GFP
1.81 0.39 1.0 0.0 0.0
100
75
α-RFP
0.0 0.39 1.0 1.81 2.29
PS
+ + + - - RPM1-EYFP
+ + + - - T7-RIN4
+ + + - - AvrRPM1-HA
- - + - + MAP-mCh-SAC1^{dead}
- + - + - MAP-mCh-SAC1^{WT}
kDa
135
α-GFP
0.85 0.62 1.0 0.0 0.0
PS
100
75
α-RFP
0.0 2.52 1.0 3.03 7.86
PS
+ + + - - RPM1-EYFP
+ + + - - T7-RIN4
+ + + - - AvrRPM1-HA
- - + - + MAP-mCh-dOCRL^{dead}
- + - + - MAP-mCh-dOCRL^{WT}
kDa
135
α-GFP
0.83 1.09 1.0 0.0 0.0
PS
75
α-RFP
0.0 0.80 1.0 4.23 4.22
PS

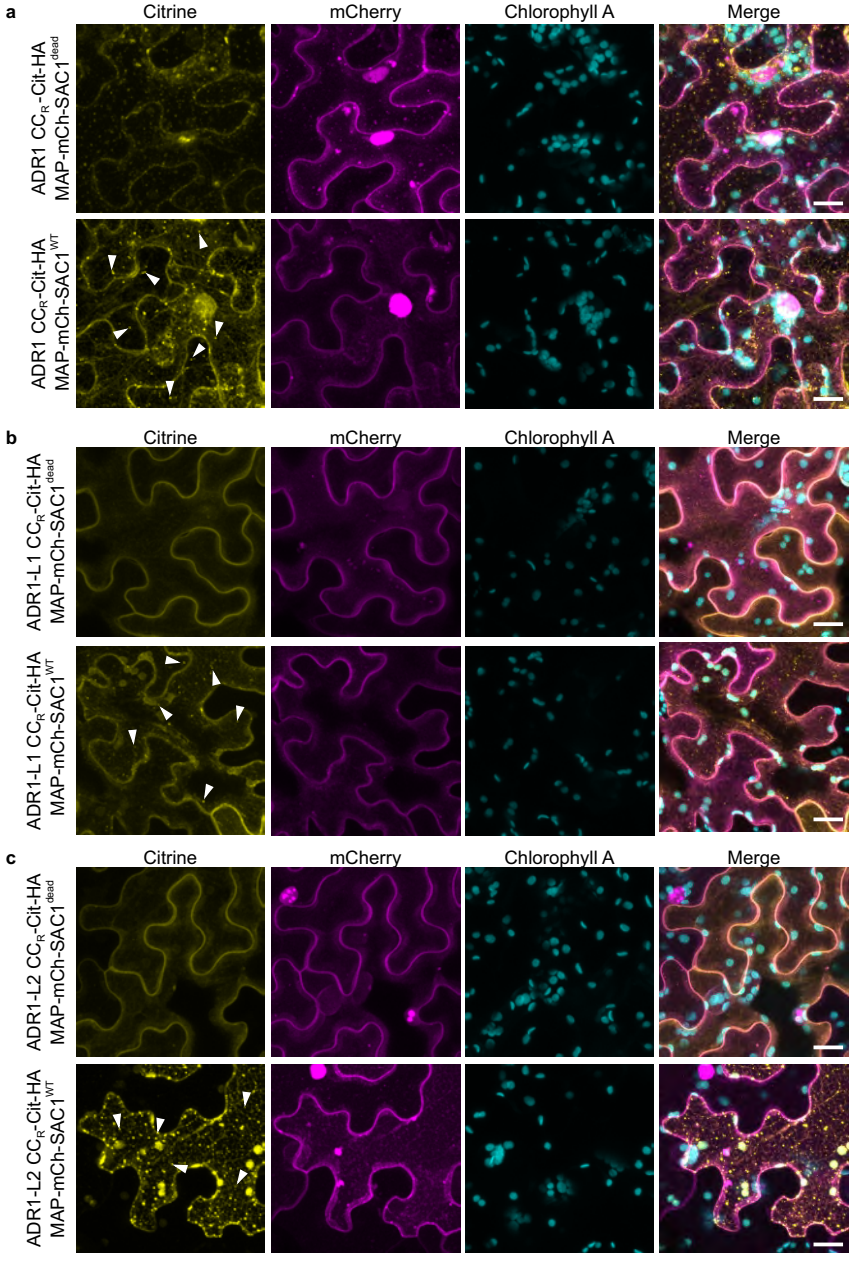
a
Citrine
mCherry
Chlorophyll A
Merge
ADR1 CC$_R$-Cit-HA
MAP-mCh-SAC1^{dead}
ADR1 CC$_R$-Cit-HA
MAP-mCh-SAC1^{WT}
b
Citrine
mCherry
Chlorophyll A
Merge
ADR1-L1 CC$_R$-Cit-HA
MAP-mCh-SAC1^{dead}
ADR1-L1 CC$_R$-Cit-HA
MAP-mCh-SAC1^{WT}
c
Citrine
mCherry
Chlorophyll A
Merge
ADR1-L2 CC$_R$-Cit-HA
MAP-mCh-SAC1^{dead}
ADR1-L2 CC$_R$-Cit-HA
MAP-mCh-SAC1^{WT}

S7 Fig.

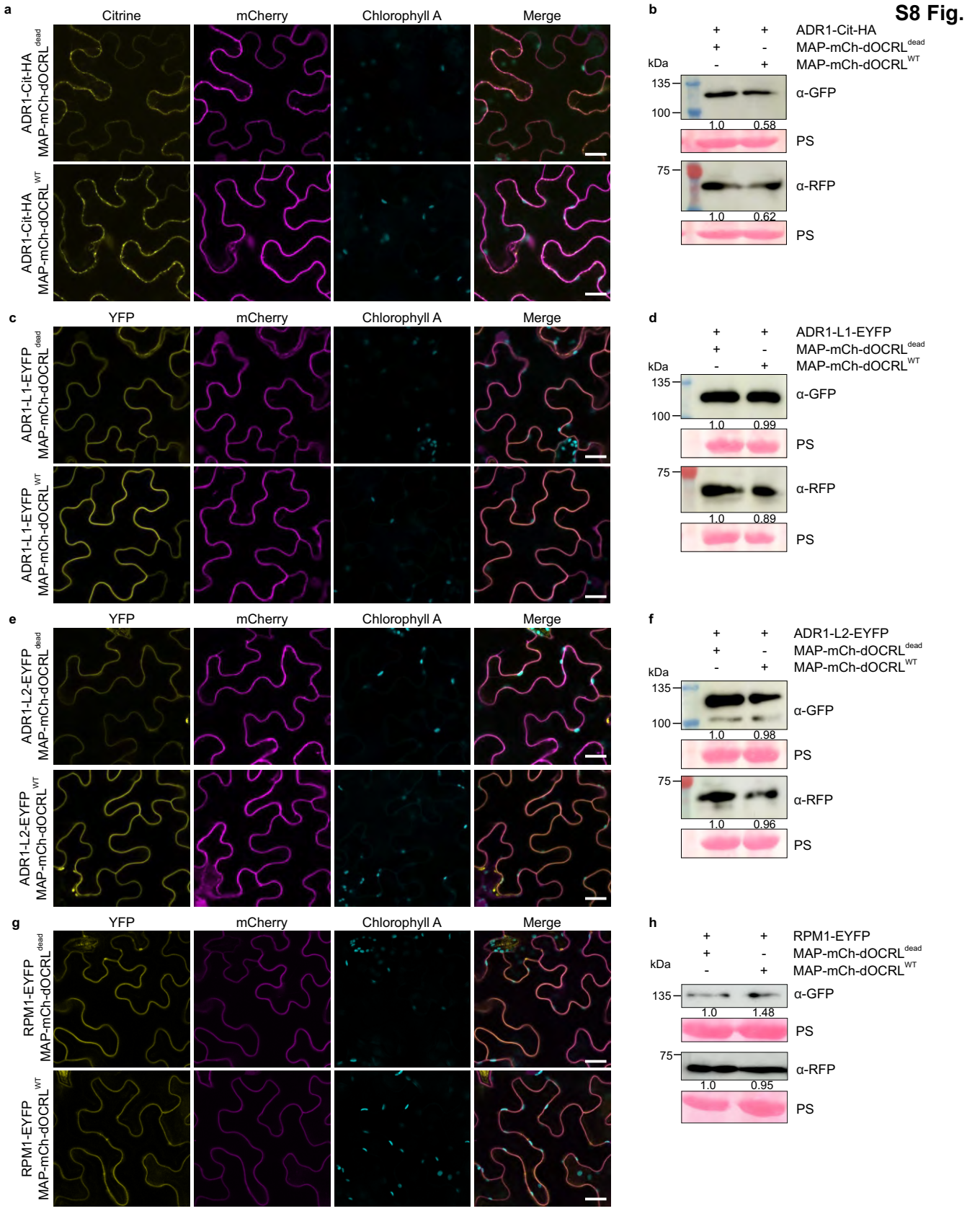
a
Citrine
mCherry
Chlorophyll A
Merge
ADR1-Cit-HA
MAP-mCh-dOCRL dead
ADR1-Cit-HA
MAP-mCh-dOCRL WT
b
ADR1-Cit-HA
MAP-mCh-dOCRL dead
MAP-mCh-dOCRL WT
kDa
135
100
1.0
0.58
α-GFP
PS
75
1.0
0.62
α-RFP
PS
c
YFP
mCherry
Chlorophyll A
Merge
ADR1-L1-EYFP
MAP-mCh-dOCRL dead
ADR1-L1-EYFP
MAP-mCh-dOCRL WT
d
ADR1-L1-EYFP
MAP-mCh-dOCRL dead
MAP-mCh-dOCRL WT
kDa
135
100
1.0
0.99
α-GFP
PS
75
1.0
0.89
α-RFP
PS
e
YFP
mCherry
Chlorophyll A
Merge
ADR1-L2-EYFP
MAP-mCh-dOCRL dead
ADR1-L2-EYFP
MAP-mCh-dOCRL WT
f
ADR1-L2-EYFP
MAP-mCh-dOCRL dead
MAP-mCh-dOCRL WT
kDa
135
100
1.0
0.98
α-GFP
PS
75
1.0
0.96
α-RFP
PS
g
YFP
mCherry
Chlorophyll A
Merge
RPM1-EYFP
MAP-mCh-dOCRL dead
RPM1-EYFP
MAP-mCh-dOCRL WT
h
RPM1-EYFP
MAP-mCh-dOCRL dead
MAP-mCh-dOCRL WT
kDa
135
1.0
1.48
α-GFP
PS
75
1.0
0.95
α-RFP
PS

S9 Fig.

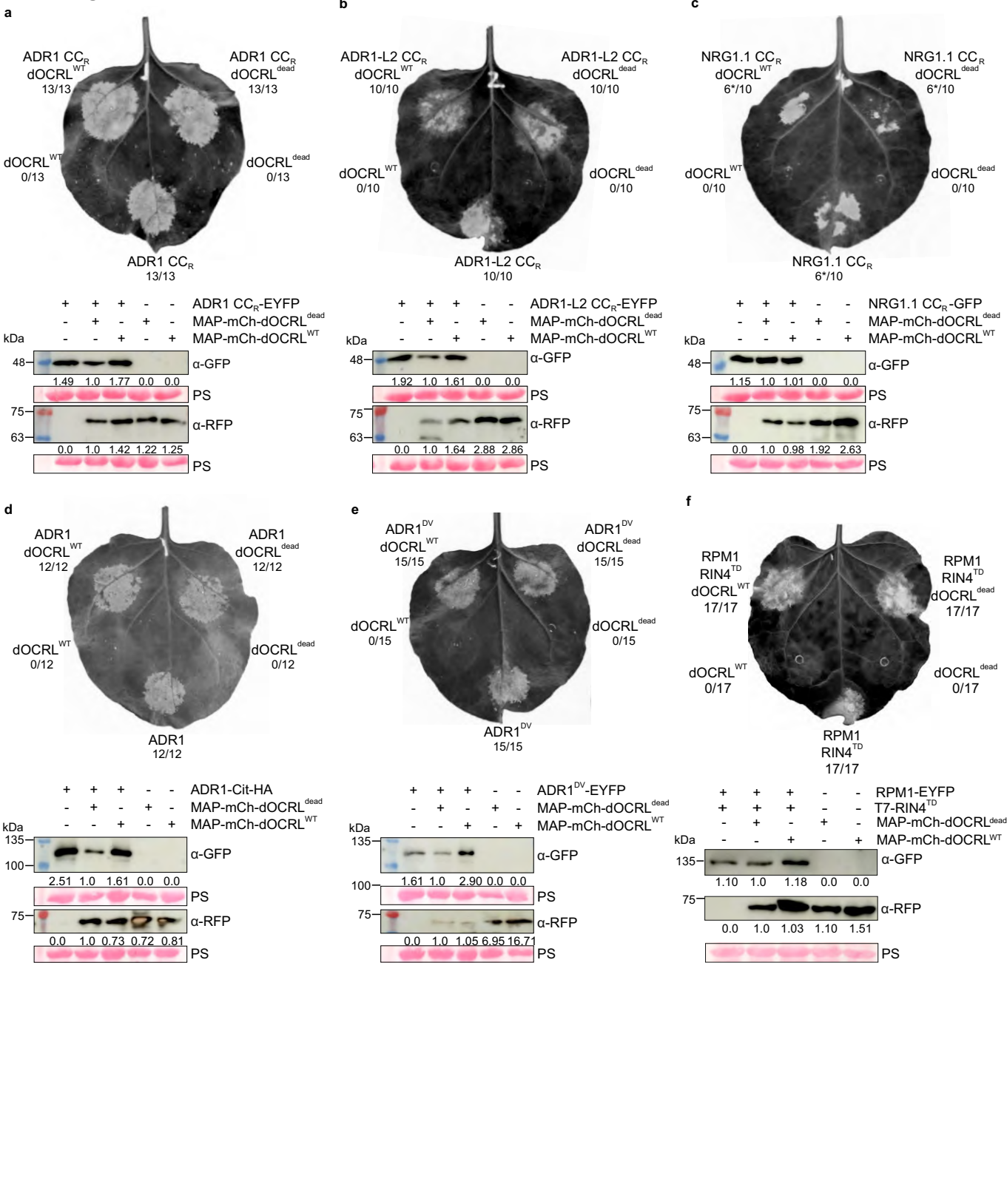
a
ADR1 CC$_R$ dOCRL^{WT} 13/13
ADR1 CC$_R$ dOCRL^{dead} 13/13
dOCRL^{WT} 0/13
dOCRL^{dead} 0/13
ADR1 CC$_R$ 13/13
+ + + - - ADR1 CC$_R$-EYFP
- + - + - MAP-mCh-dOCRL^{dead}
kDa - - + - + MAP-mCh-dOCRL^{WT}
48 α-GFP
1.49 1.0 1.77 0.0 0.0
PS
75 α-RFP
63
0.0 1.0 1.42 1.22 1.25
PS
b
ADR1-L2 CC$_R$ dOCRL^{WT} 10/10
ADR1-L2 CC$_R$ dOCRL^{dead} 10/10
dOCRL^{WT} 0/10
dOCRL^{dead} 0/10
ADR1-L2 CC$_R$ 10/10
+ + + - - ADR1-L2 CC$_R$-EYFP
- + - + - MAP-mCh-dOCRL^{dead}
kDa - - + - + MAP-mCh-dOCRL^{WT}
48 α-GFP
1.92 1.0 1.61 0.0 0.0
PS
75 α-RFP
63
0.0 1.0 1.64 2.88 2.86
PS
c
NRG1.1 CC$_R$ dOCRL^{WT} 6*/10
NRG1.1 CC$_R$ dOCRL^{dead} 6*/10
dOCRL^{WT} 0/10
dOCRL^{dead} 0/10
NRG1.1 CC$_R$ 6*/10
+ + + - - NRG1.1 CC$_R$-GFP
- + - + - MAP-mCh-dOCRL^{dead}
kDa - - + - + MAP-mCh-dOCRL^{WT}
48 α-GFP
1.15 1.0 1.01 0.0 0.0
PS
75 α-RFP
63
0.0 1.0 0.98 1.92 2.63
PS
d
ADR1 dOCRL^{WT} 12/12
ADR1 dOCRL^{dead} 12/12
dOCRL^{WT} 0/12
dOCRL^{dead} 0/12
ADR1 12/12
+ + + - - ADR1-Cit-HA
- + - + - MAP-mCh-dOCRL^{dead}
kDa - - + - + MAP-mCh-dOCRL^{WT}
135 α-GFP
100
2.51 1.0 1.61 0.0 0.0
PS
75 α-RFP
0.0 1.0 0.73 0.72 0.81
PS
e
ADR1^{DV} dOCRL^{WT} 15/15
ADR1^{DV} dOCRL^{dead} 15/15
dOCRL^{WT} 0/15
dOCRL^{dead} 0/15
ADR1^{DV} 15/15
+ + + - - ADR1^{DV}-EYFP
- + - + - MAP-mCh-dOCRL^{dead}
kDa - - + - + MAP-mCh-dOCRL^{WT}
135 α-GFP
100
1.61 1.0 2.90 0.0 0.0
PS
75 α-RFP
0.0 1.0 1.05 6.95 16.71
PS
f
RPM1 RIN4^{TD} dOCRL^{WT} 17/17
RPM1 RIN4^{TD} dOCRL^{dead} 17/17
dOCRL^{WT} 0/17
dOCRL^{dead} 0/17
RPM1 RIN4^{TD} 17/17
+ + + - - RPM1-EYFP
+ + + - - T7-RIN4^{TD}
- + - + - MAP-mCh-dOCRL^{dead}
kDa - - + - + MAP-mCh-dOCRL^{WT}
135 α-GFP
1.10 1.0 1.18 0.0 0.0
75 α-RFP
0.0 1.0 1.03 1.10 1.51
PS

S10 Fig.

Figure S10

(a)

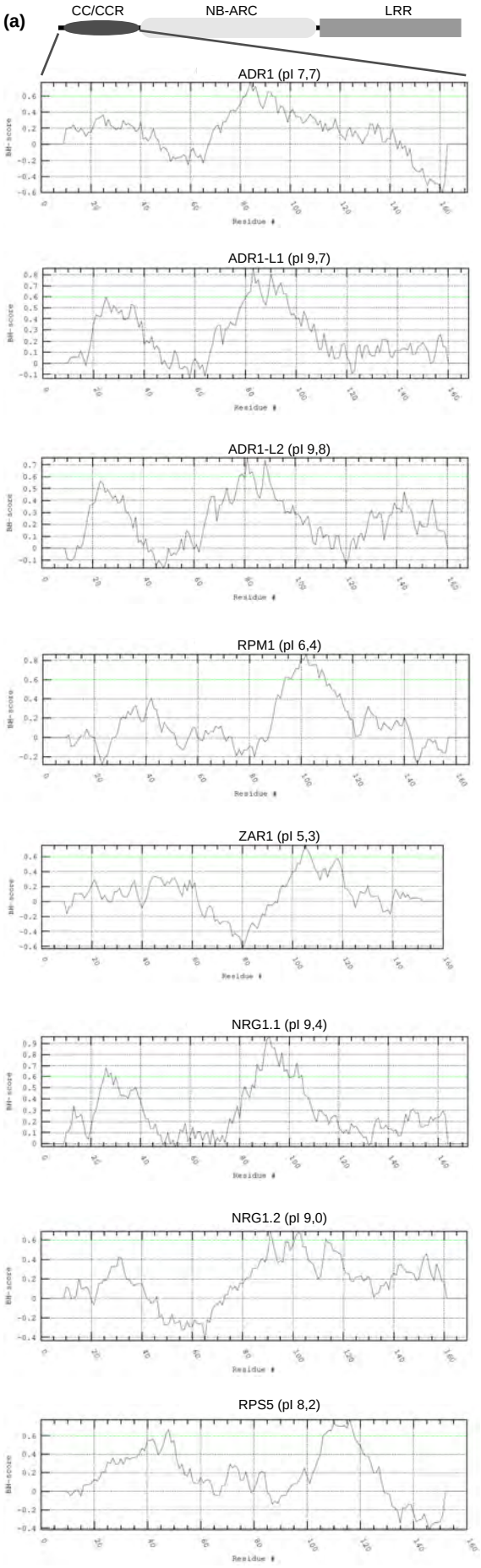

(b)

>AT1g33560_ADR1

MASFIDLFAGDITTQLLKLLALVANTVYSCKGIAERLIT
MIRDVQPTIREIQYSGAELSNHHQTQLGVFYEILEKAR
KLCE*KVLRCNRWNLKHV*YHANKMKDLEKQISRFLNS
QILLFVLAEVCHLRVNGDRIERNMDRLLTERNDSLSFP
ETMMEIETV

>AT4g33300_ADR1-L1

MAITDFFAGEIATELLKQLFTISTTAWRYKNTAKQLLTL
IDSIRPTIKEIQYSGVELPAHRQAQIGMLFDTLEKGKKL
TD*KVLSSKRWNLYRQLTL*ARKMEKLEKTISNFLKNEV
FTHILADVHHLRADTSVRLDRVDMSLDRVIQQVGSMK
IGGGGLIS

>AT5g04720_ADR1-L2

MADIIGGEVVTELVRQLYAVSQKTLRCRGIAKNLATMI
DGLQPTIKEIQYSGVELTPHRQAQLRMFSETLDKCRK
LTE*KVLKSSRWNMVRQ*LLHVRKMENLQSKVSSFLNG
QLLVHVLADVHHVRADSEFRFDRIDRKVDSLNEKLGS
MKLRGSESLREALKTAEATV

>At3g07040_RPM1

MASATVDFGIGRILSVLENETLLLSGVHGEIDKMKKEL
LIMKSFLEDTHKHGGNGSTTTTQLFQTFVANTRDLA
YQIEDILDEFGYHIHGYR*SCAKIWRAFHFPRYMW*ARH
SIAQKLGMVNVMIQSISDSMKRYYHSENYQAALLPPID
DGDAKWVNNI

>AT3g50950_ZAR1

MVDAVVTVFLEKTLNILEEKGRTVSDYRKQLEDLQSE
LKYMQSFLKDAERQKRTNETLRTLVADLRELVYEAED
ILVDCQLADGDDGNEQRSSNAWLSRLH*PARVPLQYK
KSKRLQEI*NERITKIKSQVEPYFEFITPSNVGRDNGTD
RWSSPVYDHTQV

>AT5g66900_NRG1.1

MNDWASLGIGSIGEAVFSKLLKVVIDEAKKFKAFKPLS
KDLVSTMEILFPLTQKIDSMQKELDFGVKELKELRDTI
ERADVAVRKF*PRVKWYEKSKYTRKIERIN*KDMLKFC
QIDLQLLQHRNQLTLLGLTGNLVNSVDGLSKRMDLLS
VPAPVFRDLCS

>AT5g66910_NRG1.2

MVVVDWLGLGLGSVAGALVSEGLKVLISEAKKVLAFK
SVSNELASTMESLLPVIKEIESMQDGMELQDLKDTIDK
ALLLVEKCSHVEKWN*IILKSKYTRKVEEIN*RKMLKFCQ
VQLQLLLFRNQLKSMPSMEAILNNYFQNINKKLDRLS
GSPAPPLVSK

>AT1g12220_RPS5

MGGCFSVSLPCDQVVSQFSQLLCVRGSYIHNLSKNL
ASLQKAMRMLKARQYDVIRRLETEEFTGRQQRLSQV
QVWLTSVLIIQNQFNDLLRSNEVELQRLCLCGF*CSKD
LKLSYRYGKR*VIMMLKEVESLSSQGFFDVVSEATPFA
DVDEIPFQPTIVGQ

S11 Fig.

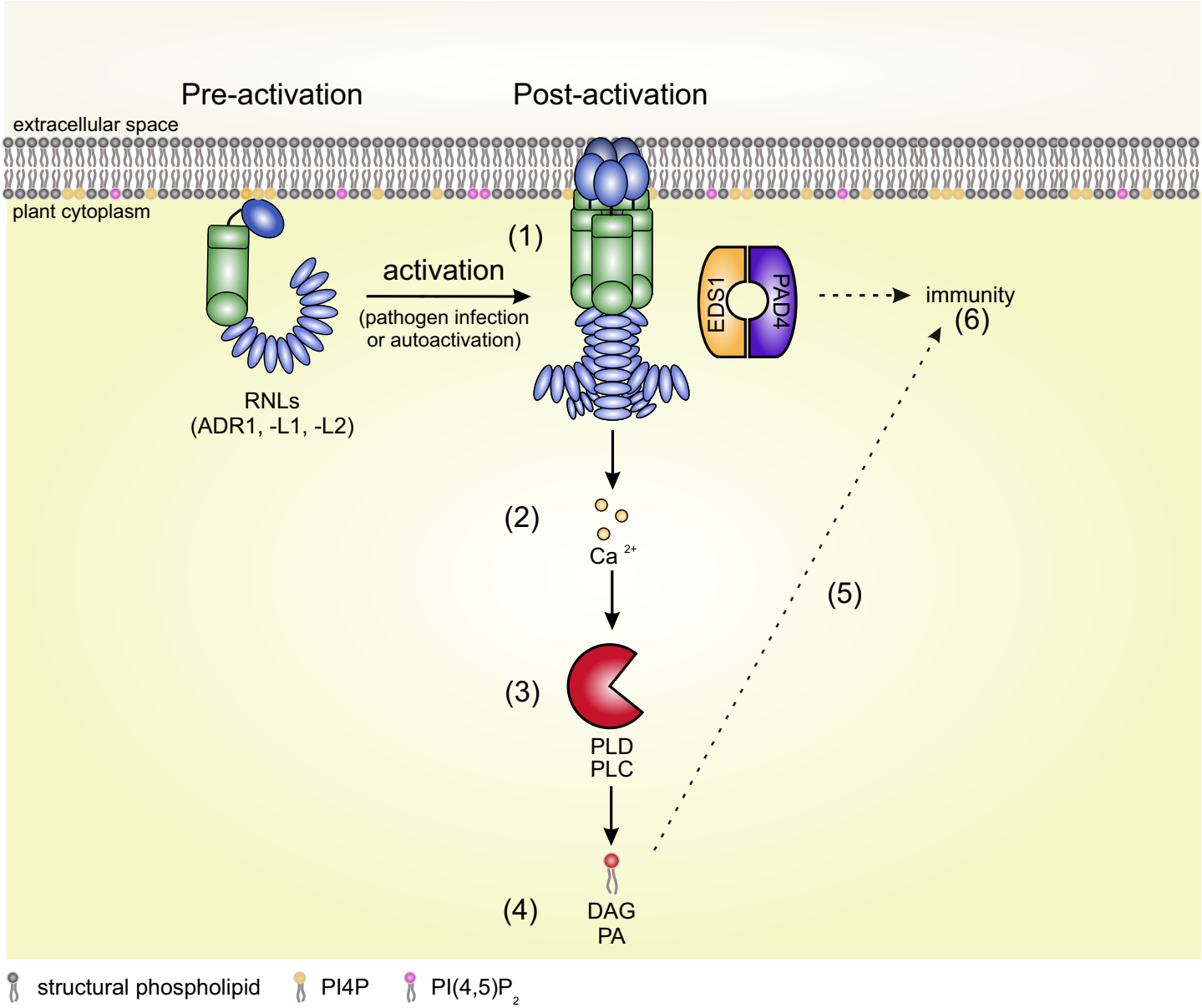
Pre-activation
Post-activation
extracellular space
plant cytoplasm
RNLs
(ADR1, -L1, -L2)
activation
(pathogen infection
or autoactivation)
(1)
EDS1
PAD4
immunity
(6)
(2)
Ca 2+
(5)
(3)
PLD
PLC
(4)
DAG
PA
structural phospholipid
PI4P
PI(4,5)P 2